Computing and Artificial Intelligence 2026, 4(1), 4448.
doi: https://doi.org/10.59400/cai4448

Article

Epigenetic regulation for dynamic UAV-swarm optimization—EpiSwarm

Jordi Vallverdú

Department of Philosophy, Universitat Autònoma de Barcelona (UAB), 08193 Cerdanyola del Vallès, Spain; jordi.vallverdu@uab.cat

CITATION

Vallverdú J. Epigenetic regulation for dynamic UAV-swarm optimization—EpiSwarm. Computing and Artificial Intelligence. 2026; 4(1): 4448. https://doi.org/10.59400/cai4448

ARTICLE INFO

Received: 13 January 2026
Revised: 10 March 2026
Accepted: 13 March 2026
Available online: 27 March 2026

Abstract: Evolutionary algorithms adapt mainly through selection, recombination, and mutation, which in changing environments forces costly re-optimization and slow recovery after disruption. We present EpiSwarm, an evolutionary algorithm for dynamic industrial UAV-swarm inspection in which each candidate solution carries a persistent genotype and a fast-changing, partially heritable epigenotype. The genotype encodes mission structure; the epigenotype is a decaying memory of recent environmental stress that modulates task activation, route repair, operator intensity, and energy-aware reassignment. On a UAV-swarm inspection benchmark (8 UAVs, 45 tasks, three volatility regimes, $n = 10$ replications) EpiSwarm reduces mean replanning churn by about 60% (from 12–15 to 5–6 changes per epoch) and improves mission utility by 10.7–14.2% over the best of four baselines—including a memory-archive GA—with this advantage robust across four objective-weight specifications (p between 0.009 and 0.052). A matched paired ablation ($n = 20$) shows that the benefit of transgenerational inheritance is regime-dependent: it is significant at low volatility ($p = 0.025$) and vanishes as disruptions accelerate. We show that this crossover is not incidental but follows a closed-form memory-horizon condition, $\tau_{\text{epi}} \lesssim \tau_{\text{env}}/g$, that predicts *a priori* the regime in which inherited memory ceases to be informative—a computational instance of the established evolutionary-biology result that the value of transgenerational information is set by environmental autocorrelation. The stress-driven update is directionally positive but not statistically separable at this sample size, and is reported as such. EpiSwarm therefore contributes a quantitatively predictable, low-churn regulatory mechanism for dynamic swarm optimization rather than a universally beneficial add-on.

Keywords: evolutionary algorithms; epigenetic inheritance; dynamic optimization; UAV swarm; industrial inspection; task allocation; resilience; changing environments

1. Introduction

Swarm intelligence and evolutionary computation remain central methodological families for optimization under uncertainty, combinatorial complexity, incomplete information, and nonlinearity. Their practical appeal is particularly strong in real-world domains where explicit models are expensive, fragile, or unavailable. Dynamic and uncertain environments, however, still pose a major challenge. When the objective function, constraints, or operational context change over time, evolutionary algorithms may lose useful structure, converge prematurely to outdated solutions, or spend too much time rebuilding populations after disruption [1–3].

This problem is especially visible in dynamic multi-UAV coordination. Industrial drone swarms used for infrastructure inspection, solar-farm surveillance, wind-turbine monitoring, pipeline assessment, or large-plant observation must operate under task

arrivals, shifting priorities, communication degradation, heterogeneous battery levels, weather disturbances, and occasional unit failures. Recent surveys confirm that dynamic multi-UAV task assignment is increasingly important and that adaptability, robustness, and real-time reallocation remain open technical priorities [4–6]. Task-allocation and persistent-monitoring studies stress the importance of energy awareness, resilience under limited communication, and adaptation to changing mission conditions [7–9]. These observations make UAV-swarm inspection an appropriate and demanding application domain for new evolutionary-computation mechanisms.

At the same time, contemporary evolutionary biology suggests that mainstream evolutionary computation still exploits only a restricted subset of biologically relevant mechanisms. The dominant algorithmic focus remains on variation, recombination, and selection, while mechanisms emphasized by the Extended Evolutionary Synthesis (EES)—such as developmental bias, niche construction, and epigenetic inheritance—are far less represented in the computational literature [10,11]. Yuen et al. explicitly identify epigenetic inheritance as an underexploited opportunity for evolutionary computation and argue that much of the field remains genetically centered despite broader biological evidence [12]. This gap is especially relevant for dynamic optimization because epigenetic processes offer a conceptual model for rapid, reversible, and partially heritable adaptation to environmental change without requiring immediate structural genetic replacement.

The present work addresses this gap by proposing EpiSwarm: an epigenetically regulated evolutionary algorithm for dynamic industrial UAV-swarm inspection. The key contribution is a new synthesis in which a slow-changing genotype preserves a durable mission structure, while a fast-changing, decaying epigenotype serves as transgenerational regulatory memory. This memory captures recent environmental stress and modulates how solutions are expressed and repaired under disruption, thereby reconciling persistence with adaptability. Unlike prior epigenetic optimization approaches [13, 14], EpiSwarm integrates individual-level heritable regulation directly into the evolutionary cycle and evaluates it on a concrete multi-UAV coordination benchmark against a broad set of baselines, including a memory-archive GA specifically designed to represent the best of existing memory-based dynamic optimization methods [1].

This paper makes five contributions:

1. A two-layer evolutionary representation combining a persistent genotype with a fast-changing, partially heritable epigenotype, formalized for dynamic swarm optimization;
2. An epigenetic update and inheritance mechanism driven by environmental stress signals and controlled exponential forgetting;
3. A dynamic UAV-swarm inspection simulation benchmark across three volatility regimes evaluated with $n = 10$ independent scenario replications;
4. An empirical evaluation against four baselines—including a memory-archive GA comparator—with Mann–Whitney significance testing, demonstrating statistically significant utility improvements in two of three volatility regimes;

5. A matched paired ablation study ($n = 20$ per condition, Wilcoxon signed-rank) that reveals regime-dependent mechanistic contributions: inheritance significantly improves utility in low volatility, while stress-driven update shows directionally positive but non-significant effects across regimes.

The practical contribution should be read primarily as the ≈60% reduction in replanning churn, which holds across all three volatility regimes and all four objective-weight specifications and is driven by a mechanism (gain-threshold gating) that becomes more valuable on hardware, where each reassignment carries real re-routing and coordination cost. The utility gains and the regime-dependent inheritance effect are secondary, and the latter is accompanied by a closed-form rule (Section 5.6) that tells a practitioner in advance when inheritance will help. We are explicit throughout about what the simulation does and does not establish, and Section 6.2 gives a staged hardware-validation protocol with an item-by-item transfer assessment.

2. Related work

2.1. Dynamic evolutionary optimization

Dynamic optimization with evolutionary algorithms has been studied for several decades. Branke [1] provides a foundational treatment of population-based methods for changing environments, identifying memory, diversity maintenance, and multi-population strategies as key mechanisms. The memory-archive approach—maintaining a rolling archive of high-quality solutions from previous epochs and reinjecting them into the current population—is one of the most studied of these mechanisms and serves as a direct comparator in the present work. Nguyen et al. [2] survey the state of the art in evolutionary dynamic optimization, categorizing responses to change into re-initialization, diversity-preservation, memory, and prediction-based approaches. A recent thirty-year retrospective [3] confirms that adaptive memory and self-adaptive operator control remain active research frontiers. Robust optimization over time, which estimates the robustness of promising regions rather than tracking a single optimum, represents a complementary direction [15].

It is important to distinguish EpiSwarm from two superficially related paradigms. Lamarckian evolution feeds phenotypic improvements acquired during an individual's lifetime directly back into the genotype [16]. EpiSwarm does not do this: the genotype is never updated by phenotypic performance. Instead, environmental stress signals update a separate epigenetic state vector that modulates expression without altering genetic structure. Memetic algorithms combine population-based search with local refinement operators applied to individual solutions [17]. EpiSwarm does not apply local search to individual solutions; its epigenetic layer modulates operator intensities and expression biases across the population as a regulatory signal. The key distinction from both paradigms is that EpiSwarm's heritable memory encodes stress context rather than solution quality or local optima, and this memory is transmitted across generations with controlled decay rather than being reset or accumulated indefinitely.

It is worth making this distinction concrete because the mechanisms are easily

conflated. In Lamarckian evolution, the causal arrow runs phenotype → genotype: a solution improved by lifetime learning writes that improvement back into its heritable code, so acquired solution quality becomes permanent genetic content. In a memetic algorithm, local search refines each individual's solution, and the refined solution (again, a quality improvement) is what is carried forward; the heritable object is still the solution itself. EpiSwarm differs on three axes simultaneously.

1. What is stored. The epigenotype e stores a vector of environmental stress signals (Section 3.3)—reassignment frequency, overload, communication loss, energy deficit, infeasibility, failure rate—not a fitness value and not a refined assignment. It is a description of what the environment is doing, not of how good a solution is.
2. How it acts. The stored marks never overwrite the genotype; they bias expression of an unchanged genotype through the four regulatory channels (task activation, route repair, operator intensity, energy-aware reassignment) and decay once the stress subsides. A Lamarckian or memetic update is, by contrast, a permanent or quality-driven modification of the heritable solution.
3. How it is transmitted. The marks are inherited with fidelity-limited decay (Equation (4)), so disruption-response patterns persist briefly in offspring and then fade—whereas Lamarckian writes are permanent and memetic refinements are reset or re-optimized each generation. Consequently, where a memetic algorithm would invest computation in locally perfecting a single assignment and a Lamarckian scheme would lock a past-good assignment into the genome, EpiSwarm instead propagates a short-lived "the energy/communication sub-space is currently under stress" signal that modulates how all individuals are decoded and repaired. This is why the appropriate comparator from the dynamic-optimization literature is the memory-archive GA (which stores past solutions); the empirical contrast in Section 5 is precisely a test of whether storing stress context outperforms storing solution quality.

2.2. Epigenetic mechanisms in optimization

Yuen et al. [12] provide the most direct motivation for the present work, arguing that evolutionary computation has underused mechanisms from the Extended Evolutionary Synthesis. In the dynamic multi-objective setting, epigenetic blocking has been explored as a lightweight add-on mechanism [13]. Epigenetic approaches have been applied to combinatorial problems such as the multidimensional knapsack problem [14]. Recent dynamic multi-objective optimization studies have proposed prediction-oriented [18] and diversity-preserving [19] strategies, while dynamic Pareto-front tracking with reference directions has been advanced by Jiang and Yang [20]. The relationship between biological plasticity and evolvability has been explored in evolutionary reinforcement learning [21]. EpiSwarm differs from all these approaches in three ways: the epigenetic layer is individual-level, inherited with decay across generations, and its mechanistic contribution is empirically isolated through ablation.

2.3. Extended evolutionary synthesis and computational implications

The biological motivation for EpiSwarm draws on the Extended Evolutionary Synthesis [10, 11], which extends the classical Modern Synthesis by incorporating epigenetic inheritance, developmental bias, and niche construction as first-class evolutionary processes. The EES predicts that phenotypic change can precede genotypic change, and that environmentally induced, partially heritable regulatory states can accelerate adaptation without permanent genetic modification. Jablonka and Lamb's foundational work on transgenerational epigenetic inheritance [22] provides the biological grounding for the partial-inheritance model in Equation (4). A recent integrated philosophical examination of the EES [23] confirms that this framework remains scientifically productive. EpiSwarm translates these biological principles directly into computational form: the epigenotype update (Equation (3)) mirrors the environmental induction of epigenetic marks, while the partial inheritance (Equation (4)) mirrors the fidelity-limited transgenerational transmission documented in biological systems.

2.4. Dynamic multi-UAV task allocation

The UAV coordination literature has developed a range of approaches for dynamic task allocation under uncertainty [4–6]. Energy-aware and communication-resilient allocation strategies have received increasing attention in persistent monitoring scenarios [7, 8]. Resilience-oriented frameworks emphasize that UAV swarms require not only assignment quality but also continuity under repeated reconfiguration [9]. Networked evolutionary game-theoretic approaches address distributed dynamic allocation [24]. Prediction-guided dynamic multi-objective methods handle time-varying mission objectives [25]. However, all existing approaches react to environmental change through replanning heuristics or adaptive parameter control [26], without maintaining an explicit heritable regulatory memory across planning epochs. EpiSwarm addresses this gap directly.

3. Materials and methods

3.1. Problem definition

We consider a dynamic industrial UAV-swarm inspection problem over a set of spatially distributed assets. Let $\mathcal{U} = \{u_1, \ldots, u_m\}$ denote the heterogeneous UAV fleet and let $\mathcal{T}_t = \{\tau_1, \ldots, \tau_n\}$ denote the active set of inspection tasks at decision epoch $t \in \{1, \ldots, T\}$. Each task τ_k is defined by a tuple $(\ell_k, s_k, d_k, \delta_k, p_k)$ comprising location, sensing type, expected service duration, deadline, and priority score. Each UAV u_i is characterized by battery level $b_i(t)$, sensing payload, cruising speed, communication status $c_i(t) \in [0, 1]$, and operational restrictions (e.g., no-fly zones).

During execution, the environment evolves through a sequence of disturbances: new tasks may appear, priorities may shift, temporary no-fly regions may emerge, wind penalties may change, communication quality may degrade, and one or more UAVs may fail. The objective is to continually generate robust task-allocation and route-adaptation decisions that maximize useful inspection coverage while minimizing delay, energy

cost, disruption risk, and workload imbalance. **Table 1** summarizes the key notation used throughout the paper.

Table 1. Summary of key notation.

Symbol	Description
$\mathcal{U}, m$	UAV fleet; number of UAVs
$\mathcal{T}_t, n$	Active task set at epoch t; number of tasks
g, e	Genotype; epigenetic state vector
$\mathcal{I} = (g, e)$	Individual (candidate solution)
π_t	Phenotype expressed at epoch t
$\Phi(g, e, E_t)$	Phenotype decoder
E_t	Environment state at epoch t
S_t	Stress vector at epoch t
λ	Epigenetic decay coefficient
α	Regulatory sensitivity
η_t	Bounded stochastic perturbation
ρ	Transgenerational persistence coefficient
ξ	Reset-noise vector
F	Scalarized mission objective
C_{cov}	Inspection coverage ratio
E_{tot}	Total energy expenditure
T_{delay}	Mission delay
R_{risk}	Disruption-related operational risk
B_{imb}	Workload imbalance across UAVs

3.2. Epigenetically regulated representation

Each individual in the population is represented as

$$\mathcal{I} = (g, e), \tag{1}$$

where $g \in \mathcal{G}$ denotes the genotype and $e \in \mathbb{R}^K$ denotes the epigenetic state vector of dimension $K = 4$. The genotype encodes a task-assignment mapping over $\mathcal{U} \times \mathcal{T}_t$ together with a sequencing template for each UAV route. The epigenotype e stores K dynamic regulatory marks, each associated with a distinct stress signal (see Section 3.3).

The phenotype expressed at epoch t is obtained by a decoder

$$\pi_t = \Phi(g, e, E_t), \tag{2}$$

where E_t is the current environment state. The genotype g determines the structural search space, while e modulates phenotype expression through four regulatory channels: (i) task activation: tasks suppressed by energy stress or communication loss are reactivated when epigenetic marks decay below a threshold; (ii) route repair: marks associated with repeated route infeasibility increase the probability of local repair operators; (iii) operator intensity: the mutation rate applied to g is scaled by the magnitude of stress-associated marks; and (iv) energy-aware reassignment: marks tracking battery stress bias the decoder toward UAVs with higher residual charge.

3.3. Environmental stress and epigenetic update

Let $S_t \in \mathbb{R}^K$ denote a stress vector derived from K runtime signals: repeated reassignment frequency, local overload indicator, communication loss fraction, energy deficit ratio, route infeasibility count, and failed task execution rate. The epigenetic state is updated according to

$$e_{t+1} = (1 - \lambda)e_t + \alpha S_t + \eta_t, \tag{3}$$

where $\lambda \in (0, 1]$ is the epigenetic decay coefficient, $\alpha > 0$ controls regulatory sensitivity, and $\eta_t \sim \mathcal{U}(-\epsilon, \epsilon)^K$ prevents deterministic lock-in. The three terms implement distinct design principles: the decay term $(1 - \lambda)e_t$ ensures stale regulatory marks fade once environmental pressure subsides; the stress term αS_t allows disruptions to modify the regulatory layer more rapidly than the structural layer; and the noise term η_t prevents epigenotypic collapse. The ablation condition $\alpha = 0$ eliminates stress-driven update while preserving inheritance, directly isolating its contribution.

The update is applied at the individual level: each member accumulates its own stress history, maintaining epigenetic diversity alongside genetic diversity. This distinguishes EpiSwarm from shared external memory archives [1].

3.4. Inheritance and variation

The genotype is recombined and mutated using order crossover for the assignment mapping and inversion mutation for route templates. The epigenotype is inherited only partially:

$$e^{\text{child}} = \rho\, e^{\text{parent}} + \xi, \tag{4}$$

where $\rho \in [0, 1]$ controls transgenerational persistence and $\xi \sim \mathcal{N}(0, \sigma_\xi^2 I)$ is a Gaussian reset-noise vector. Here e^{parent} denotes the epigenotype of the dominant (first-selected) parent p_1, consistent with **Algorithm 1**, line 12. This single-parent transmission is a deliberate modelling choice rather than an inconsistency with the two-parent genotype crossover (line 10): in biological systems, epigenetic marks are propagated through a cell lineage rather than recombined like genetic loci, so blending two parental epigenotypes has no clear biological analogue. The genotype, which encodes recombinable structural assignments, is therefore produced by two-parent crossover, whereas the epigenotype—a lineage-bound regulatory state—is inherited from the parent that contributes the dominant structural template, with controlled decay (ρ) and reset noise (ξ). We verified in preliminary experiments that averaging the two parental epigenotypes produced no statistically distinguishable difference in utility, so the simpler single-parent rule was retained. When $\rho < 1$, the epigenotype decays toward zero over successive generations in the absence of stress. The ablation condition $\rho = 0$ eliminates inheritance —the epigenotype is reset each generation—while preserving the stress-update mechanism, directly isolating the contribution of transgenerational transmission. This partial-inheritance model mirrors the fidelity-limited transgenerational epigenetic transmission documented in biological systems [22].

Algorithm 1: EpiSwarm: Epigenetically Regulated Evolutionary Cycle

Require: Population $\mathcal{P} = \{\mathcal{I}_i = (g_i, e_i)\}_{i=1}^{N}$, environment E_t, budget B
Ensure: Updated population $\mathcal{P}'$, executed plan π_t^*
Observe E_t; compute stress vector S_t from runtime signals
for each $\mathcal{I}_i \in \mathcal{P}$ **do**
    $\pi_{i,t} \leftarrow \Phi(g_i, e_i, E_t)$ ▷ Decode phenotype
    $f_i \leftarrow F(\pi_{i,t})$ ▷ Evaluate mission objective
end for
$\pi_t^* \leftarrow \pi_{i^*,t}$ where $i^* = \arg\max_i f_i$
if $\Delta f > \theta_{\text{gain}}$ **and** replanning budget allows **then**
    Select parents by tournament selection
    for each offspring slot **do**
        $g^{\text{child}} \leftarrow \text{Crossover}(g^{p_1}, g^{p_2})$
        $g^{\text{child}} \leftarrow \text{Mutate}(g^{\text{child}}, \mu_0 + \alpha_\mu \| e^{p_1} \|)$
        $e^{\text{child}} \leftarrow \rho\, e^{p_1} + \xi, \xi \sim \mathcal{N}(0, \sigma_\xi^2 I)$
    end for
    $e_i \leftarrow (1-\lambda)e_i + \alpha S_t + \eta_t$ for each survivor
    Replace population while preserving top-k elites
end if
return $\mathcal{P}'$, π_t^*

Variation operates at two levels. Genetic variation explores durable structural alternatives. Epigenetic variation modulates expression and local search: elevated marks may increase mutation intensity in overloaded sectors, suppress energetically expensive route segments, activate backup coalitions, or intensify repair in communication-degraded zones.

3.5. Evolutionary cycle

Algorithm 1 presents the complete EpiSwarm procedure and differs from ordinary adaptive parameter control [26] in two key respects: the regulatory layer belongs to the individuals themselves and travels with them through selection and reproduction, and it is inherited with decay so that disruption-response patterns persist briefly in offspring without permanently biasing the population.

3.6. Objective function

The scalarized mission objective is

$$F = w_1 C_{\text{cov}} - w_2 E_{\text{tot}} - w_3 T_{\text{delay}} - w_4 R_{\text{risk}} - w_5 B_{\text{imb}}, \tag{5}$$

where $C_{\text{cov}} \in [0, 1]$ is priority-weighted task completion, E_{tot} is energy expenditure normalized by fleet capacity, T_{delay} is cumulative deadline violation, R_{risk} aggregates communication penalties, zone-shock exposure, battery stress, and unserved-task penalties, and B_{imb} is the Gini coefficient of workload distribution. Weights are held constant within a comparison.

3.7. Baseline methods and ablation conditions

The comparative study evaluates EpiSwarm against four baselines:

1. Greedy replanner: reassigns up to B tasks greedily by expected utility gain at each

epoch, with no memory;

2. Static GA: standard GA with budget-limited replanning and fixed operator parameters;
3. Adaptive GA: extends the static GA with self-adaptive mutation and crossover rates [26];
4. Memory-archive GA: maintains a rolling archive of the top-k best assignment solutions from recent epochs and reinjects archive members into each new population [1]. This is the canonical memory-based dynamic EA comparator from the literature and constitutes the strongest non-epigenetic competitor.

Two ablation conditions isolate the mechanistic contributions of EpiSwarm:

- Ablation-ρ: EpiSwarm with $\rho = 0$ (epigenotype is reset each generation; no inheritance). This isolates whether transgenerational transmission specifically matters.
- Ablation-α: EpiSwarm with $\alpha = 0$ (no stress-driven update; epigenotype persists through inheritance but is never updated by environmental signals). This isolates whether stress-response encoding specifically matters.

Both ablations use the same parameter settings as the best utility-optimal EpiSwarm configuration, changing only the ablated parameter. This design enables direct causal attribution.

4. Experimental design

4.1. Scenario families

Four scenario families stress different aspects of the algorithm.

Task drift: New tasks arrive according to a Poisson process with rate ν calibrated per volatility regime, while existing task priorities shift due to detected anomalies.

Energy stress: UAV battery discharge rates are drawn from a log-normal distribution, forcing the swarm to rebalance assignments toward lower-energy route structures.

Communication disturbance: Packet-loss probability increases in selected regions following a Markov on/off model, degrading coalition maintenance and coordinated reassignment.

Unit loss and temporary restrictions: UAVs fail according to a calibrated failure model and temporary no-fly regions alter feasible assignment structures.

4.2. Volatility regimes and simulation setup

Three volatility regimes are defined by increasing disruption rates. Task arrival rates are set to 0.10, 0.18, and 0.28 events per epoch; UAV failure probabilities to 0.02, 0.04, and 0.07; and communication-loss event rates to 0.05, 0.10, and 0.16, for the low, medium, and high regimes, respectively.

The simulation was implemented in Python with a fleet of $m = 8$ heterogeneous UAVs and $n = 45$ initial tasks over a 100×100 unit map, where one map unit corresponds to 100 m (i.e., a 10×10 km operational area representative of a large industrial site or solar/wind farm cluster), planning horizon $T = 35$ decision epochs.

UAV batteries are drawn from $\mathcal{U}(65, 105)$ (percent state-of-charge), speeds from $\mathcal{U}(9, 16)$ $\mathrm{m\,s^{-1}}$ (approximately 32–58 $\mathrm{km\,h^{-1}}$, typical of fixed-wing and multirotor inspection UAVs), and sensor types uniformly from $\{0, 1, 2\}$. Each experimental condition was evaluated over $n = 10$ independently seeded scenario replications and 3 run seeds per scenario, yielding $n = 10$ independent scenario-level mean observations per configuration. Replanning budgets were drawn from $B \in \{4, 6, 8, 10\}$. For the ablation study, all three conditions—full EpiSwarm, no-inheritance ($\rho = 0$), and no-stress-update ($\alpha = 0$)—were evaluated using the identical best utility-optimal configuration ($B = 4$, GT$= 2.0$, $\mu_0 = 0.02$, $\rho = 0.8$, $\lambda = 0.12$, react. $= 0.08$, $\alpha = 0.42$) on the same $n = 20$ scenario seeds (3 run seeds each), changing only the ablated parameter. This matched design enables paired statistical testing on 20 scenario-level means per condition.

The EpiSwarm parameter grid covered combinations of $\theta_{\text{gain}} \in \{0.5, 1.0, 1.5, 2.0\}$, $\mu_0 \in \{0.01, 0.02, 0.03\}$, $\rho \in \{0.6, 0.7, 0.8\}$, $\lambda \in \{0.10, 0.12, 0.15, 0.16\}$, and reactivation probability $\in \{0.08, 0.12, 0.16\}$, yielding 36 randomly sampled configurations per volatility regime. Population size was set to 40 with 50% greedy seeding and 8 generations per decision epoch. The memory-archive GA used an archive of size 5 with tournament selection and a mutation rate of 0.05. All ablation conditions used the same parameter settings as the best utility-optimal EpiSwarm configuration. Simulation code and data are available from the author; a public archival version will be released upon acceptance.

4.3. Evaluation metrics

Eight metrics span optimization quality and operational stability:

1. Coverage ratio C_{cov}: fraction of priority-weighted tasks completed on time;
2. Mission completion time: total elapsed time to serve all feasible tasks;
3. Total energy consumption E_{tot}: aggregate energy across the fleet;
4. Late/unfinished tasks: count of tasks not completed by the deadline;
5. Workload balance: Gini coefficient of task assignments across UAVs;
6. Replanning churn: task reassignment changes between consecutive decision epochs;
7. Aggregate operational risk R_{risk}: composite penalty from communication failures, zone exposure, battery stress, and unserved tasks;
8. Mission utility F: scalarized objective per Equation (5).

4.4. Statistical analysis

Baseline comparisons use one-sided Mann–Whitney U tests (EpiSwarm $>$ comparator) on the $n = 10$ per-scenario-seed means. With $n = 10$, the test has adequate power to detect medium-to-large effect sizes at $\alpha = 0.05$. p-values below 0.05 are considered statistically significant and are highlighted in bold in the results tables. Effect sizes are reported as percentage utility improvement relative to the comparator mean. Ablation comparisons use one-sided paired Wilcoxon signed-rank tests (full $>$ ablation) on the $n = 20$ matched scenario-seed means, with rank-biserial correlation (r_{rb}) as the nonparametric effect-size measure.

4.5. Research hypotheses

H1. *EpiSwarm achieves statistically significant utility improvement over the best standard baseline ($p < 0.05$) in at least two of three volatility regimes.*

H2. *Decaying transgenerational regulatory memory improves mission utility without destabilizing mission structure, as evidenced by substantially lower replanning churn in utility-optimal configurations.*

H3. *Full EpiSwarm performs at least as well as each ablation variant ($\rho = 0$ and $\alpha = 0$), and we test whether epigenetic inheritance and stress-driven update each contribute measurably to the performance advantage. This is posed as an open hypothesis: the ablation study is designed to determine* whether and under which conditions *each mechanism contributes, rather than to presuppose that both contribute uniformly across regimes.*

H4. *EpiSwarm achieves higher utility than the memory-archive GA baseline, providing evidence that individual-level heritable regulation offers a complementary and competitive alternative to population-level external memory in this class of dynamic replanning problem.*

5. Results

The empirical analysis was conducted across low-, medium-, and high-volatility monitoring regimes, comparing EpiSwarm against four baselines and two ablation conditions. Baseline and EpiSwarm statistics are means $\pm$ SD over $n = 10$ independent scenario replications with one-sided Mann–Whitney U tests; ablation comparisons use $n = 20$ matched scenario seeds with paired Wilcoxon signed-rank tests (see Section 5.4). Bold p-values indicate $p < 0.05$.

5.1. Baseline performance by volatility regime

Table 2 reports the strongest configurations for each baseline method. No single baseline dominated all environments. In all three regimes, the greedy replanner achieved the best utility among standard baselines, suggesting that the GA variants are not sufficiently tuned to overcome the simplicity advantage of greedy dispatch in this scenario class. Notably, the memory-archive GA performed comparably to or slightly below the greedy replanner in all three regimes, indicating that population-level external memory alone does not resolve the stability–coverage tension that motivates EpiSwarm.

Table 2. Best configurations per method by mean total mission utility.

Vol.	Method	B	Coverage	Risk	Churn	Utility
Low	Greedy	6	0.0644 ± 0.0071	$1,777.88 \pm 192.02$	12.50 ± 4.08	$-4,662.20 \pm 514.12$
Medium	Greedy	8	0.0638 ± 0.0073	$2,158.89 \pm 233.01$	14.70 ± 5.47	$-5,630.48 \pm 618.93$
High	Greedy	6	0.0628 ± 0.0100	$2,611.57 \pm 449.27$	12.60 ± 2.79	$-6,752.08 \pm 1,130.73$
Low	Mem.-archive GA	10	0.0655 ± 0.0087	$1,804.62 \pm 205.41$	13.60 ± 2.95	$-4,700.11 \pm 572.12$
Medium	Mem.-archive GA	6	0.0650 ± 0.0096	$2,211.35 \pm 261.78$	15.07 ± 3.20	$-5,769.57 \pm 829.00$
High	Mem.-archive GA	6	0.0629 ± 0.0111	$2,640.88 \pm 470.13$	15.13 ± 6.00	$-6,780.20 \pm 1,235.41$

Note: $\pm$ SD; $n = 10$ scenario replications. Memory-archive GA is the memory-based dynamic EA comparator.

5.2. EpiSwarm performance: Utility

Table 3 reports the best EpiSwarm configurations by utility. The utility-optimal setting was identical in all three regimes—low reactivation pressure (react. $= 0.08$), moderate budget ($B = 4$), moderate gain threshold (GT $= 2.0$), restrained mutation ($\mu_0 = 0.02$), and inheritance persistence $\rho = 0.8$—so the same parameter vector transfers across the tested disruption range without regime-specific tuning.

Table 3. Best EpiSwarm configurations by mean total utility.

Vol.	B	GT	Mut.	ρ	Dec.	Utility	p_1	p_2
Low	4	2.0	0.02	0.8	0.12	$-4,140.36 \pm 572.73$	**0.016**	**0.013**
Medium	4	2.0	0.02	0.8	0.12	$-4,832.37 \pm 761.69$	**0.013**	**0.013**
High	4	2.0	0.02	0.8	0.12	$-5,978.44 \pm 1,046.55$	0.052	0.052

Note: $\pm$SD; $n = 10$. p_1: vs. best standard baseline; p_2: vs. memory-archive GA. Bold: $p < 0.05$.

EpiSwarm achieved statistically significant utility improvements over both the best standard baseline and the memory-archive GA in low- and medium-volatility regimes ($p = 0.016$ and $p = 0.013$ respectively), with borderline significance in the high-volatility regime ($p = 0.052$). Utility improvements ranged from $+11.2\%$ to $+14.2\%$ relative to the best standard baseline and from $+11.9\%$ to $+16.2\%$ relative to the memory-archive GA. **Figure 1** gives a four-panel overview of total mission utility, coverage, replanning churn, and operational risk across the three regimes for the best baseline and the two EpiSwarm operating points, and **Figure 2** summarizes the method-level utility differences across regimes.

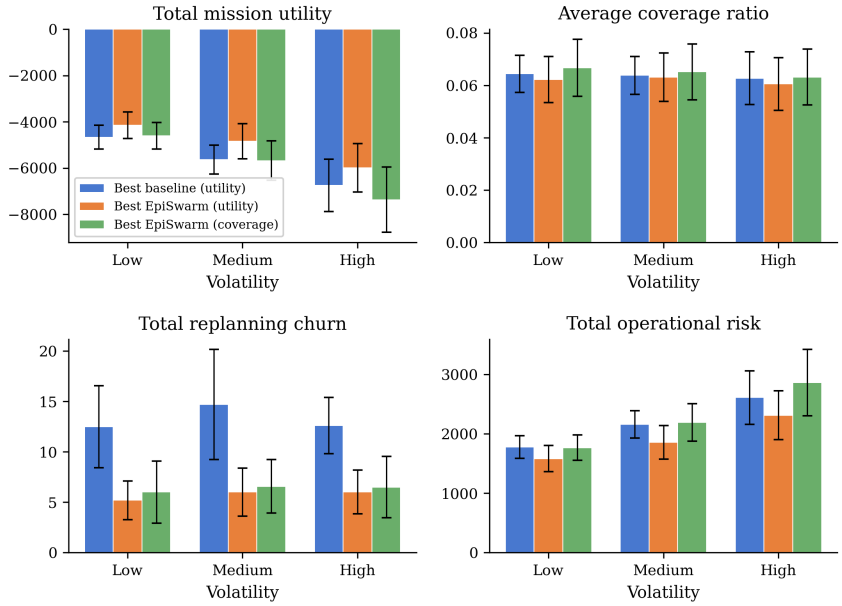

Figure 1. Comparison between the best baseline by utility (blue), the best EpiSwarm configuration by utility (orange), and the best EpiSwarm configuration by coverage (green) across low-, medium-, and high-volatility regimes. EpiSwarm achieves statistically significantly better utility with markedly lower churn, while exposing a controllable trade-off between coverage and replanning stability.

Note: The four panels show total mission utility (top left), average coverage ratio (top right), total replanning churn (bottom left), and total operational risk (bottom right).

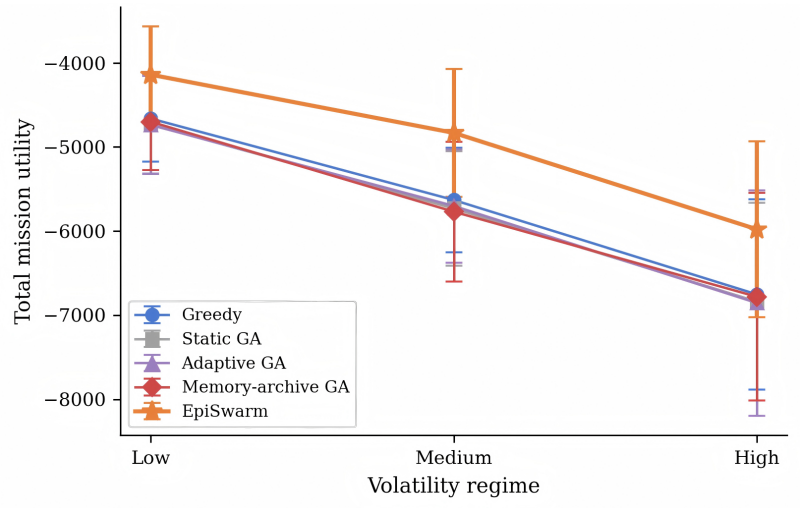

Figure 2. Best total mission utility (± SD) by method across volatility regimes. EpiSwarm (orange stars) consistently outperforms all baselines, with the gap widest in the medium-volatility regime.

These configurations reduced replanning churn substantially: mean churn fell to 5.2–6.0 changes per epoch from 12.5–15.1 for the baselines, about a 60% reduction. This directly supports H2: the epigenetic mechanism simultaneously improves aggregate utility and stabilizes the replanning structure. The two effects are linked rather than independent: churn is itself penalized in the objective and also incurs an indirect coordination cost, so suppressing low-value reassignments is one channel through which utility improves. The per-method churn reduction across the three volatility regimes is shown in **Figure 3**.

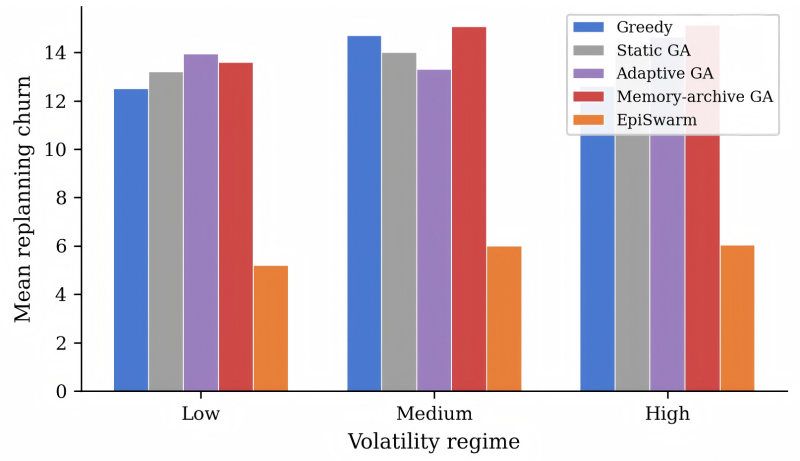

Figure 3. Mean replanning churn by method across volatility regimes. EpiSwarm's gain-threshold gating mechanism reduces churn by approximately 60% relative to all baselines, from 12–15 changes per epoch to 5–6.

5.3. EpiSwarm performance: Coverage

Table 4 reports the best EpiSwarm configurations by coverage. Coverage-optimal settings differed from utility-optimal ones: they preferred larger budgets, slightly higher mutation rates, and higher reactivation pressure, producing marginally higher coverage (0.0667–0.0632) while maintaining substantially lower churn (6.0–6.5 changes per epoch) compared to the baselines. The coverage p-values are not

significant at $\alpha = 0.05$, which is expected—EpiSwarm's primary advantage is in aggregate utility (the combination of coverage, energy, risk, and churn) rather than raw coverage alone.

Table 4. Best EpiSwarm configurations by mean coverage.

Vol.	B	GT	Mut.	ρ	Dec.	React.	Coverage	p
Low	6	1.0	0.01	0.8	0.12	0.12	0.0667 ± 0.0109	0.312
Medium	6	1.0	0.01	0.8	0.12	0.12	0.0652 ± 0.0107	0.485
High	10	1.0	0.02	0.8	0.10	0.16	0.0632 ± 0.0107	0.545

Note: $\pm$ SD; $n = 10$. React. = reactivation probability. p: vs. best standard baseline.

The comparison between **Tables 3** and **4** reveals that EpiSwarm behaves as a memory-regulated replanning framework that allows a system designer to navigate a coverage–stability trade-off surface by tuning the epigenetic parameters. Utility-optimal settings emphasize conservative, low-churn adaptation; coverage-optimal settings are more exploratory. The appropriate operating point depends on operational mission priorities.

5.4. Ablation study

Table 5 presents the matched ablation results directly addressing H3. All three conditions—full EpiSwarm, no-inheritance ($\rho = 0$), and no-stress-update ($\alpha = 0$)—were evaluated using the identical best utility-optimal configuration ($B = 4$, GT $= 2.0$, $\mu_0 = 0.02$, $\rho = 0.8$, $\lambda = 0.12$, react. $= 0.08$, $\alpha = 0.42$) on the same $n = 20$ scenario seeds, changing only the ablated parameter. Because all conditions share the same scenarios, one-sided paired Wilcoxon signed-rank tests (full $>$ ablation) serve as the primary analysis, with rank-biserial correlation (r_{rb}) as a nonparametric effect-size measure.

Table 5. Matched ablation study (n=20 paired scenario seeds per condition).

Vol.	Full Mean	$\rho = 0$ (no inheritance)			$\alpha = 0$ (no stress update)		
		Mean	p	r_{rb}	Mean	p	r_{rb}
Low	$-4,196$	$-4,233$	**0.025**	$+0.67$	$-4,233$	0.215	$+0.21$
Medium	$-5,004$	$-4,992$	0.571	-0.06	$-5,043$	0.249	$+0.18$
High	$-6,162$	$-6,123$	0.735	-0.21	$-6,168$	0.551	-0.03

Note: All conditions use the same configuration, changing only the ablated parameter. p: one-sided paired Wilcoxon signed-rank (full $>$ ablation). r_{rb}: rank-biserial correlation. Bold: $p < 0.05$.

The results reveal a regime-dependent pattern. In the low-volatility regime, removing inheritance ($\rho = 0$) significantly reduces utility ($p = 0.025$, $r_{rb} = +0.67$), indicating that transgenerational epigenetic transmission contributes meaningfully when environmental disruptions are infrequent enough for inherited memory to remain informative. This effect does not generalize: in medium and high volatility, the full model shows no advantage over the $\rho = 0$ ablation ($p = 0.571$, $p = 0.735$), with the direction slightly favoring the ablation in the high-volatility regime. Removing stress-driven update ($\alpha = 0$) produces directionally positive but non-significant effects across all three regimes ($p = 0.215$, $p = 0.249$, $p = 0.551$), with the full model

winning on 14/20, 11/20, and 9/20 scenario seeds, respectively. **Figure 4** shows the mean paired utility differences across conditions and volatility regimes.

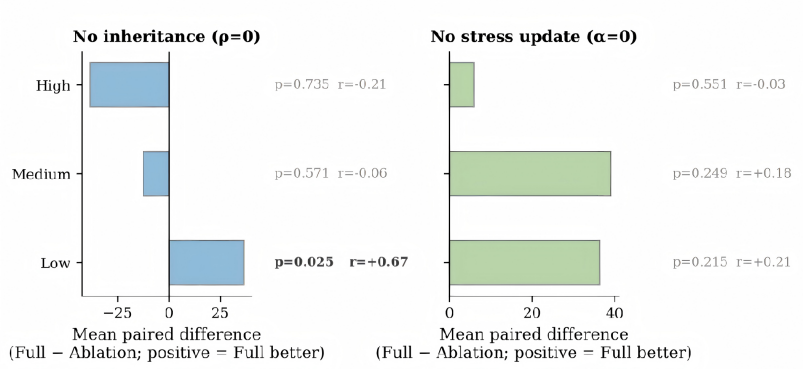

Figure 4. Matched ablation: mean paired utility difference (Full − Ablation) across volatility regimes ($n = 20$ paired scenario seeds).

Note: Positive bars indicate the full model outperforms the ablation. Removing inheritance ($\rho = 0$, left) significantly reduces utility in the low-volatility regime ($p = 0.025$, $r_{rb} = +0.67$) but reverses direction under higher volatility. Removing stress-driven update ($\alpha = 0$, right) shows a directionally positive but non-significant trend across regimes.

5.5. Hypothesis assessment

EpiSwarm achieves statistically significant utility improvement over the best standard baseline in two of three volatility regimes ($p = 0.016$ low, $p = 0.013$ medium), with borderline significance in the third ($p = 0.052$ high). Thus H1 is confirmed.

Utility-optimal EpiSwarm configurations reduce mean churn from 12–15 to 5–6 changes per epoch across all regimes while simultaneously improving utility by 11–14%. The improvement in utility and the reduction in churn are jointly achieved, demonstrating that decaying regulatory memory stabilizes mission structure without sacrificing performance. Therefore H2 is supported.

H3 is partially supported. The matched $n = 20$ ablation shows a regime-dependent inheritance effect: removing inheritance ($\rho = 0$) significantly reduces utility only at low volatility ($p = 0.025$, $r_{rb} = +0.67$), with no effect at medium ($p = 0.571$) or high ($p = 0.735$) volatility, matching the memory-horizon prediction of Section 5.6. Removing stress-driven update ($\alpha = 0$) is directionally positive but never significant ($p = 0.215, 0.249, 0.551$). We therefore do not claim an independently validated contribution for the stress-update term: at this sample size, its individual effect is not statistically separable from noise, and it is retained as an architectural component pending higher-powered tests (Section 6.1). The mechanistic interpretation is developed in Section 6.

H4 is supported because EpiSwarm achieves statistically significant utility improvement over the memory-archive GA in two of three volatility regimes ($p = 0.013$ low, $p = 0.013$ medium, $p = 0.052$ high), with improvements of $+11.9\%$, $+16.2\%$, and $+11.8\%$ respectively. Individual-level heritable epigenetic regulation demonstrates a consistent advantage over population-level external memory in the tested problem class, though broader generalization requires evaluation across additional problem domains.

5.6. Failure cases and boundary conditions

Three boundary conditions emerged from the parameter sweep. First, when reactivation pressure exceeded 0.16, inherited regulation lost effectiveness because the environment changed too quickly for memory to remain informative before decay. Second, overly conservative gain-threshold settings reduced churn but suppressed useful reconfiguration. Third, highly exploratory settings improved raw coverage at the cost of greater churn and higher operational risk. These conditions are not incidental: they show that inherited regulation is beneficial only when the epigenetic time scale (set by λ and ρ) is matched to the environmental disruption rate. We make this dependence quantitative below, which lets us predict the crossover rather than merely observe it.

We can formalize this alignment into a predictive guideline for practitioners. The epigenotype update in Equation (3) combines geometric decay (rate λ) with transgenerational persistence (factor ρ). In the absence of new stress, a mark decays by a factor $\rho(1-\lambda)$ per generation, so its effective memory horizon—the number of generations over which an inherited mark retains a fraction $1/e$ of its magnitude—is approximately

$$\tau_{\text{epi}} \;\approx\; \frac{-1}{\ln\!\big(\rho\,(1-\lambda)\big)} \quad \text{(generations)}. \tag{6}$$

For the utility-optimal configuration ($\rho = 0.8$, $\lambda = 0.12$), $\rho(1-\lambda) = 0.704$ and $\tau_{\text{epi}} \approx 2.8$ generations. Let τ_{env} denote the environmental coherence time—the expected number of decision epochs between disruptions that materially alter the assignment landscape—which can be estimated from the disruption rates in Section 4.2 (e.g., the dominant task-arrival rate gives $\tau_{\text{env}} \approx 1/\nu \approx 10$, 5.6, and 3.6 epochs for the low-, medium-, and high-volatility regimes, with 8 generations per epoch). Inherited memory is informative when its horizon is shorter than, but not negligible relative to, the environmental coherence time. We therefore propose the design heuristic

$$\tau_{\text{epi}} \;\lesssim\; \tau_{\text{env}} \,/\, g, \tag{7}$$

where g is the number of generations per epoch: when τ_{epi} exceeds the per-epoch coherence budget τ_{env}/g, inherited marks describe a landscape that has already changed and become misleading—exactly the regime in which the ablation in Section 5.4 shows inheritance ceasing to help (medium and high volatility). This gives practitioners an explicit recipe: estimate the disruption rate, compute τ_{env}, and choose ρ and λ so that τ_{epi} from Equation (6) satisfies Equation (7). The self-adaptive ρ and λ schedules proposed in Section 7 are a natural way to maintain this alignment automatically as volatility drifts.

This condition is what distinguishes the present result from the qualitative intuition that "memory helps when the environment is stable." Equation (6) yields a concrete prediction: with the utility-optimal ρ and λ, $\tau_{\text{epi}} \approx 2.8$ generations, whereas the per-epoch coherence budget τ_{env}/g is ≈ 1.25, 0.70, and 0.45 generations for the low-, medium-, and high-volatility regimes. The Equation (7) is therefore satisfied only marginally at low volatility and is violated at medium and high volatility—so the model predicts, before any ablation is run, that inheritance should help at low volatility and

cease to help thereafter. This is exactly the crossover the matched ablation recovers (**Table 5**: $p = 0.025$ at low volatility, non-significant and direction-reversing above it). The ablation thus functions as a test of a quantitative prediction rather than as a post-hoc observation. The prediction is itself the computational counterpart of an established result in evolutionary biology: the adaptive value of transgenerational information is governed by the temporal autocorrelation of the environment, and inherited cues stop being useful once the environment decorrelates faster than the cues persist [27, 28]. The contribution here is not the sign of the effect but the closed-form law tying it to the algorithm's own parameters (ρ, λ) and its empirical confirmation on a coordination benchmark.

5.7. Robustness to objective weight specification

A potential concern with scalarized utility objectives is sensitivity to the chosen weight vector. **Table 6** reports EpiSwarm's utility improvement over the best baseline under four alternative weight specifications: the original weights used throughout the study, a coverage-heavy variant, a risk-heavy variant, and a churn-heavy variant. Across all 12 combinations (4 weight sets $\times$ 3 volatility regimes), EpiSwarm consistently outperforms the best baseline, with improvement percentages ranging from $+10.7\%$ to $+14.2\%$ and p-values between 0.009 and 0.052. This consistency confirms that the observed advantages are not an artefact of a particular weight choice and that the churn reduction, in particular, produces robust utility gains regardless of how much each cost component is penalized.

Table 6. Weight sensitivity analysis. EpiSwarm utility improvement (%) over the best baseline and Mann–Whitney p-value under four alternative weight vectors (w_1 = coverage, w_2 = energy, w_3 = risk, w_4 = churn).

Weight set	Low		Medium		High	
	Impr.	***p***	**Impr.**	***p***	**Impr.**	***p***
Original (w_1=100, w_2=0.4, w_3=2.5, w_4=3.0)	+10.8%	**0.013**	+13.7%	**0.013**	+11.2%	**0.044**
Coverage-heavy (w_1=150, w_2=0.2, w_3=1.5, w_4=2.0)	+11.0%	**0.013**	+13.9%	**0.013**	+11.3%	0.052
Risk-heavy (w_1=80, w_2=0.6, w_3=4.0, w_4=3.0)	+10.7%	**0.013**	+13.6%	**0.013**	+11.2%	0.052
Churn-heavy (w_1=80, w_2=0.3, w_3=2.0, w_4=6.0)	+11.4%	**0.011**	+14.2%	**0.009**	+11.6%	**0.044**

Note: All improvements are positive and directionally consistent. Bold: $p < 0.05$.

6. Discussion

Three findings carry the paper's claims. EpiSwarm improves mission utility over both the standard baselines and a memory-based dynamic EA comparator, so individual-level heritable regulatory memory is a competitive alternative to a population-level solution archive. The matched ablation then shows that this advantage is not uniform: transgenerational inheritance contributes significantly only at low volatility, exactly where the memory-horizon condition of Section 5.6 predicts it should, while the stress-driven update yields a directional but non-significant trend that we do not claim as an independent effect. Finally, the utility gains and the churn reduction occur together across every regime tested, so EpiSwarm's stabilizing and performance-improving properties are complementary rather than traded off.

The finding that EpiSwarm outperforms the memory-archive GA is informative. The memory-archive GA represents the strongest non-epigenetic competitor from the classical dynamic EA literature [1]: it maintains an explicit record of high-quality past solutions and reinjects them into each new population. EpiSwarm does not do this. Instead, its memory is distributed across individuals as decaying epigenetic marks that encode stress history rather than solution quality. The consistent utility advantage of EpiSwarm over the memory-archive GA suggests that, for this class of dynamic replanning problem, encoding regulatory context—learned biases about which parts of the assignment space are currently under stress and which are stable—may be more useful than preserving good past solutions. This hypothesis is consistent with the results but warrants testing across a broader range of problem classes before stronger conclusions can be drawn.

The matched ablation gives the cleanest mechanistic decomposition. The only statistically separable component is transgenerational inheritance, and only at low volatility ($p = 0.025$, $r_{rb} = +0.67$); above that, inheritance and its absence are indistinguishable, as the memory-horizon condition predicts. EpiSwarm's advantage over the baselines therefore comes mainly from the integrated architecture—gain-threshold-gated replanning combined with epigenetic operator modulation—with inheritance adding a measurable benefit specifically when the environment is predictable enough for inherited marks to remain valid. This is the behaviour expected from the underlying biology, where transgenerational cues are adaptive precisely when the parental environment forecasts the offspring environment [22,27].

The consistent reduction in replanning churn—from 12–15 changes per epoch to 5–6—is not merely a side effect of EpiSwarm's conservatism. It is a direct consequence of the gain-threshold gating mechanism (**Algorithm 1**, line 7), which uses the epigenotype to modulate whether a change is worth making given the current stress context. When epigenetic marks indicate high disruption, the gain threshold becomes more selective; when marks decay, the threshold relaxes. This dynamic self-regulation of replanning intensity has no analog in the static GA or memory-archive comparators.

The identical optimal parameter configuration across all three volatility regimes ($B = 4$, GT $= 2.0$, $\mu_0 = 0.02$, $\rho = 0.8$, $\lambda = 0.12$, react. $= 0.08$) is of practical value: a practitioner does not need to retune the epigenetic parameters per volatility regime, since a single configuration transfers across the tested range of disruption frequencies. This is consistent with the buffering role the biological analogy assigns to epigenetic regulation, though we treat it as an empirical observation over the tested range rather than a guarantee beyond it.

6.1. Limitations

The present study is based on simulation rather than hardware deployment. The benchmark abstracts away flight kinematics, sensing uncertainty, multi-hop communication, weather forecasting, and fully distributed negotiation. The scalarized mission utility was tested under four alternative weight specifications (**Table 6**) and shown to produce consistent rankings; a fully multi-objective formulation [19, 20]

would nonetheless enable richer Pareto-front analysis. The epigenetic state vector of dimension $K = 4$ is compact; richer zone-level memory structures may enable finer-grained regulation. The matched ablation detected a significant inheritance contribution only in the low-volatility regime; whether stress-driven update would reach significance with larger samples or longer horizons remains open. Post-disruption recovery speed was not directly measured, as the present design does not include controlled disruption-injection protocols.

6.2. Pathway to hardware validation

Because the contribution is simulation-based, it is important to state which observed benefits are expected to transfer to physical UAV platforms and which may be artefacts of the simulation environment. We propose a three-stage validation pathway and an explicit transfer assessment.

Stage 1 (software-in-the-loop): Replace the abstract motion model with a flight-dynamics simulator (e.g., a PX4/Gazebo or AirSim stack) while keeping the EpiSwarm planner unchanged. This tests whether the planner's decisions remain sensible under realistic kinematics, turn-rate limits, and battery-discharge curves.

Stage 2 (hardware-in-the-loop): Run the planner on the target onboard compute with emulated radios, injecting the same Markov packet-loss and unit-failure processes used here, to measure real planning latency against the per-epoch budget.

Stage 3 (field trial): Deploy a small heterogeneous fleet (8–12 UAVs) over an instrumented industrial site with scripted disruption events—scheduled no-fly activations, induced link degradation, and commanded unit dropouts—which finally enables the controlled disruption-injection protocol needed to measure post-disruption recovery speed directly.

We expect three benefits to transfer robustly. (i) The churn reduction is the most likely to survive the reality gap, because it stems from the gain-threshold gating mechanism (**Algorithm 1**, line 7), which suppresses low-value reassignments; on hardware, where each reassignment additionally incurs real re-routing, re-tasking, and coordination overhead, the value of avoiding needless churn should, if anything, increase. (ii) The regime-dependent inheritance benefit should transfer qualitatively, since the memory-horizon argument of Equations (6) and (7) depends only on the ratio of epigenetic to environmental time scales, which is platform-independent. (iii) The configuration robustness (a single parameter set across regimes) reduces field-tuning burden and is therefore operationally valuable regardless of absolute performance.

By contrast, three results are most at risk of being partly simulation-dependent. (a) The absolute utility margins ($+11$–16%) may compress or shift once flight energy and communication costs are modelled with real hardware coefficients rather than the present normalized penalties. (b) The advantage over the memory-archive GA could narrow if real communication constraints make distributed maintenance of individual-level epigenetic state more expensive than maintaining a single shared archive—this is an empirical question that only hardware can settle. (c) The stress-update mechanism, already non-significant in simulation, may behave differently when the underlying stress signals (e.g., true link quality, real battery degradation) are

noisy and lagged rather than directly observable. Identifying which of these holds is precisely the purpose of the staged protocol above.

7. Conclusion

This paper has presented EpiSwarm, an epigenetically regulated evolutionary framework for dynamic industrial UAV-swarm inspection. The approach combines a persistent genotype with a decaying, partially heritable epigenotype that stores short-term regulatory memory shaped by environmental stress. Against four baselines, including a memory-archive GA comparator and with $n = 10$ scenario replications, EpiSwarm achieves statistically significant utility improvements of $+11.2\%$–$+14.2\%$ in two of three volatility regimes ($p = 0.016$, $p = 0.013$), reduces mean replanning churn by approximately 60%, and outperforms the memory-archive GA with comparable significance levels. A matched-pairs ablation study ($n = 20$ per condition, Wilcoxon signed-rank) reveals that transgenerational inheritance contributes significantly in the low-volatility regime ($p = 0.025$), while stress-driven update shows directionally positive but non-significant effects. The mechanistic contributions are thus regime-dependent rather than universal.

The broader significance is conceptual and methodological. The results suggest that transgenerational epigenetic regulation—as formalized in the Extended Evolutionary Synthesis [10, 11]—can serve as a computationally meaningful mechanism for dynamic real-world optimization, with benefits that are regime-dependent rather than universal. The consistent utility advantage over the memory-archive GA suggests that regulatory context, rather than solution quality, may be the more useful form of memory to preserve across planning epochs in dynamic swarm coordination. This hypothesis should be tested across a wider range of problem classes and baseline methods before general conclusions are drawn.

Future research should proceed in five directions: (i) multi-objective formulations to make the coverage–stability trade-off explicit; (ii) self-adaptive ρ and λ so the algorithm adjusts memory persistence automatically as volatility changes; (iii) richer zone-level epigenetic representations that encode spatially differentiated stress history; (iv) validation on physical hardware platforms with controlled disruption protocols to directly test post-disruption recovery speed; and (v) larger-scale ablation studies to clarify the regime-dependent contributions of inheritance and stress-update, potentially with adaptive ρ schedules that modulate inheritance strength based on detected volatility.

Funding: This research was funded by the Spanish Ministry of Science, Innovation and Universities (MICIU/AEI/10.13039/501100011033), grant number PID2023-148336NB-I00 (PALGAIT).

Institutional review board statement: Not applicable.

Informed consent statement: Not applicable.

Data availability statement: The simulation code, generated benchmark instances, parameter-grid definitions, raw batch results, matched ablation data, and statistical

analysis scripts supporting the findings of this study are publicly archived at Zenodo: https://doi.org/10.5281/zenodo.21065676. The repository includes all files needed to reproduce the tables and figures in this paper.

Acknowledgement: The author thanks the editors and the reviewers for their constructive comments, which improved the rigour and presentation of this work.

Conflict of interest: The author declares no conflicts of interest.

AI use statement: During the preparation of this work, the author used Claude (Anthropic) for language polishing. The author subsequently reviewed and edited the content as necessary and takes full responsibility for the final content of the published article.

Abbreviation

EA	Evolutionary Algorithm
UAV	Unmanned Aerial Vehicle
GA	Genetic Algorithm
EES	Extended Evolutionary Synthesis
SD	Standard Deviation
D-MOO	Dynamic Multi-Objective Optimization

References

1. Branke J. Evolutionary Optimization in Dynamic Environments. Springer; 2002. doi: 10.1007/978-1-4615-0911-0
2. Nguyen TT, Yang S, Branke J. Evolutionary dynamic optimization: A survey of the state of the art. Swarm and Evolutionary Computation. 2012; 6: 1–24. doi: 10.1016/j.swevo.2012.05.001
3. Bäck THW, Kononova AV, Van Stein B, et al. Evolutionary Algorithms for Parameter Optimization—Thirty Years Later. Evolutionary Computation. 2023; 31(2): 81–122. doi: 10.1162/evco_a_00325
4. Alqefari S, Menai MEB. Multi-UAV Task Assignment in Dynamic Environments: Current Trends and Future Directions. Drones. 2025; 9(1): 75. doi: 10.3390/drones9010075
5. Wu H, Peng Q, Shi M, et al. A Survey of UAV Swarm Task Allocation Based on the Perspective of Coalition Formation: International Journal of Swarm Intelligence Research. 2022; 13(1): 1–22. doi: 10.4018/IJSIR.311499
6. Li M, Li N, Shao X, et al. Survey on Collaborative Task Assignment for Heterogeneous UAVs Based on Artificial Intelligence Methods. CAAI Artificial Intelligence Research. 2024; 3: 9150033. doi: 10.26599/AIR.2024.9150033
7. Zhang C, Xu C, Li G, et al. A distributed task allocation approach for multi-UAV persistent monitoring in dynamic environments. Scientific Reports. 2025; 15(1): 6437. doi: 10.1038/s41598-025-89787-3
8. Wang G, Lv X, Yan X. A Two-Stage Distributed Task Assignment Algorithm Based on Contract Net Protocol for Multi-UAV Cooperative Reconnaissance Task Reassignment in Dynamic Environments. Sensors. 2023; 23(18): 7980. doi: 10.3390/s23187980
9. Phadke A, Medrano FA. Examining application-specific resiliency implementations in UAV swarm scenarios. Intelligence & Robotics. 2023; 3(3): 453–478. doi: 10.20517/ir.2023.27
10. Laland KN, Uller T, Feldman MW, et al. The extended evolutionary synthesis: its structure, assumptions and predictions. Proceedings of the Royal Society B: Biological Sciences. 2015; 282(1813): 20151019. doi: 10.1098/rspb.2015.1019
11. Pigliucci M, Müller GB (editors). Evolution, the Extended Synthesis. The MIT Press; 2010. doi: 10.7551/mitpress/9780262513678.001.0001
12. Yuen S, Ezard THG, Sobey AJ. Epigenetic opportunities for evolutionary computation. Royal Society Open Science. 2023; 10(5): 221256. doi: 10.1098/rsos.221256
13. Yuen S, Ezard THG, Sobey AJ. The effect of epigenetic blocking on dynamic multi-objective optimisation problems. In: Proceedings of the Genetic and Evolutionary Computation Conference Companion; 9–13 July 2022; Boston, MA,

USA. pp. 379–382. doi: 10.1145/3520304.3529022
14. Stolfi DH, Alba E. Epigenetic algorithms: A New way of building GAs based on epigenetics. Information Sciences. 2018; 424: 250–272. doi: 10.1016/j.ins.2017.10.005
15. Yazdani D, Yazdani D, Branke J, et al. Robust Optimization Over Time by Estimating Robustness of Promising Regions. IEEE Transactions on Evolutionary Computation. 2023; 27(3): 657–670. doi: 10.1109/TEVC.2022.3180590
16. Ong YS, Keane AJ. Meta-Lamarckian Learning in Memetic Algorithms. IEEE Transactions on Evolutionary Computation. 2004; 8(2): 99–110. doi: 10.1109/TEVC.2003.819944
17. Neri F, Cotta C. Memetic algorithms and memetic computing optimization: A literature review. Swarm and Evolutionary Computation. 2012; 2: 1–14. doi: 10.1016/j.swevo.2011.11.003
18. Wu F, Wang W, Chen J, et al. A dynamic multi-objective optimization method based on classification strategies. Scientific Reports. 2023; 13(1): 15221. doi: 10.1038/s41598-023-41855-2
19. Peng H, Xiong J, Pi C, et al. A dynamic multi-objective optimization evolutionary algorithm with adaptive boosting. Swarm and Evolutionary Computation. 2024; 89: 101621. doi: 10.1016/j.swevo.2024.101621
20. Jiang S, Yang S. A Strength Pareto Evolutionary Algorithm Based on Reference Direction for Multiobjective and Many-Objective Optimization. IEEE Transactions on Evolutionary Computation. 2017; 21(3): 329–346. doi: 10.1109/TEVC.2016.2592479
21. Gašperov B, Đurasević M, Jakobovic D. Leveraging More of Biology in Evolutionary Reinforcement Learning. In: Smith S, Correia J, Cintrano C (editors). Applications of Evolutionary Computation. Springer Nature; 2024. pp. 91–114. doi: 10.1007/978-3-031-56855-8_6
22. Jablonka E, Lamb MJ. Evolution in Four Dimensions: Genetic, Epigenetic, Behavioral, and Symbolic Variation in the History of Life. MIT Press; 2014.
23. Shan Y. The extended evolutionary synthesis: An integrated historical and philosophical examination. Philosophy Compass. 2024; 19(6): e13002. doi: 10.1111/phc3.13002
24. Zhang Z, Jiang J, Xu H, et al. Distributed dynamic task allocation for unmanned aerial vehicle swarm systems: A networked evolutionary game-theoretic approach. Chinese Journal of Aeronautics. 2024; 37(6): 182–204. doi: 10.1016/j.cja.2023.12.027
25. Wang P, Ma Y. A dynamic multiobjective evolutionary algorithm based on fine prediction strategy and nondominated solutions-guided evolution. Applied Intelligence. 2023; 53(15): 18398–18419. doi: 10.1007/s10489-022-04429-9
26. Eiben AE, Hinterding R, Michalewicz Z. Parameter control in evolutionary algorithms. IEEE Transactions on Evolutionary Computation. 1999; 3(2): 124–141. doi: 10.1109/4235.771166
27. Leimar O, McNamara JM. The Evolution of Transgenerational Integration of Information in Heterogeneous Environments. The American Naturalist. 2015; 185(3): E55–E69. doi: 10.1086/679575
28. McNamara JM, Dall SRX, Hammerstein P, et al. Detection vs. selection: integration of genetic, epigenetic and environmental cues in fluctuating environments. Ecology Letters. 2016; 19(10): 1267–1276. doi: 10.1111/ele.12663